Original Article
http://dx.doi.org/10.5115/acb.2016.49.3.189
pISSN 2093-3665 eISSN 2093-3673
Anatomy & Cell Biology acb

Rhus verniciflua Stokes attenuates cholestatic liver cirrhosis-induced interstitial fibrosis via Smad3 down-regulation and Smad7 up-regulation

Mi Na Gil[1], Du Ri Choi[1], Kwang Sik Yu[1], Ji Heun Jeong[1], Dong-Ho Bak[2], Do-Kyung Kim[1], Nam-Seob Lee[1], Je-Hun Lee[1], Young-Gil Jeong[1], Chun Soo Na[3], Dae Seung Na[3], Ki-Hyun Ryu[4], Seung Yun Han[1,5]

[1]Department of Anatomy, Konyang University College of Medicine, Daejeon, [2]Department of Dermatology, Chung-Ang University R&D Center, Seoul, [3]Lifetree Co., Ltd., Suwon, [4]Department of Gastroenterology and Hepatology, Konyang University Hospital, Daejeon, [5]Myunggok Research Institute, Konyang University College of Medicine, Daejeon, Korea

Abstract: Cholestatic liver cirrhosis (CLC) eventually proceeds to end-stage liver failure by mediating overwhelming deposition of collagen, which is produced by activated interstitial myofibroblasts. Although the beneficial effects of *Rhus verniciflua* Stokes (RVS) on various diseases are well-known, its therapeutic effect and possible underlying mechanism on interstitial fibrosis associated with CLC are not elucidated. This study was designed to assess the protective effects of RVS and its possible underlying mechanisms in rat models of CLC established by bile duct ligation (BDL). We demonstrated that BDL markedly elevated the serological parameters such as aspartate aminotransferase, alanine transaminase, total bilirubin, and direct bilirubin, all of which were significantly attenuated by the daily uptake of RVS (2 mg/kg/day) for 28 days (14 days before and after operation) via intragastric route. We observed that BDL drastically induced the deterioration of liver histoarchitecture and excessive deposition of extracellular matrix (ECM), both of which were significantly attenuated by RVS. In addition, we revealed that RVS inhibited BDL-induced proliferation and activation of interstitial myofibroblasts, a highly suggestive cell type for ECM production, as shown by immunohistochemical and semi-quantitative detection of α-smooth muscle actin and vimentin. Finally, we demonstrated that the anti-fibrotic effect of RVS was associated with the inactivation of Smad3, the key downstream target of a major fibrogenic cytokine, i.e., transforming growth factor β (TGF-β). Simultaneously, we also found that RVS reciprocally increased the expression of Smad7, a negative regulatory protein of the TGF-β/Smad3 pathway. Taken together, these results suggested that RVS has a therapeutic effect on CLC, and these effects are, at least partly, due to the inhibition of liver fibrosis by the downregulation of Smad3 and upregulation of Smad7.

Key words: *Rhus verniciflua* Stokes, Cholestatic liver cirrhosis, Bile duct ligation

Received August 18, 2016; Revised September 2, 2016; Accepted September 6, 2016

Introduction

Cholestatic liver cirrhosis (CLC) is one of the major causative factors for the development of liver fibrosis worldwide [1]. Many researchers are trying to understand the pathophysiologic mechanisms of ongoing liver fibrosis because CLC produces imponderable socio-economical costs [2]. Liver fibrosis is known as the pathologic condition involving excessive production and deposition of extracellular matrix (ECM) that originates from a wide variety of liver parenchymal cells

Corresponding authors:
Ki-Hyun Ryu
Department of Gastroenterology and Hepatology, Konyang University Hospital, Konyang University College of Medicine, 158 Gwanjeodong-ro, Seo-gu, Daejeon 35365, Korea
Tel: +82-42-600-9127, Fax: +82-42-600-9095, E-mail: medidrug@kyuh.ac.kr
Seung Yun Han
Department of Anatomy, Konyang University College of Medicine, 158 Gwanjeodong-ro, Seo-gu, Daejeon 35365, Korea
Tel: +82-42-600-6466, Fax: +82-42-600-6314, E- mail: jjzzy@konyang.ac.kr

including hepatic stellate cells (HSC), hepatocytes, endothelial cells, and cholangiocytes [3-5]. Following hepatic damage, transforming growth factor-β (TGF-β), a master inflammatory/fibrogenic cytokine, is released from infiltrating macrophages. Upon the stimulation by TGF-β, Smad3 is phosphorylated, translocate to the nucleus, and start to exert the transcription activity [6]. While the Smad3 and the Smad7, a major negative regulatory protein, keeps balance, breakdown of balance between Smad3 and Smad7 stimulates the parenchymal cells and induces their transdifferentiation into myofibroblasts [7-9]. Subsequently, ECM starts to accumulate in the interstitial space, resulting the progressive and irreversible substitution of normal parenchyma by scar tissue [10, 11].

Based on the notion that chronic inflammation essentially precedes the development of liver fibrosis, plant extracts that exert anti-inflammatory property have been empirically used for treating patients with various liver diseases in Asian countries [12]. Among them, *Rhus verniciflua* Stokes (RVS) has been traditionally used as a food supplement or a pharmaceutical in Korea and China [13]. Recent studies have revealed that RVS has various biological properties including antioxidant, antiobesity, antioncogenic, tumoricidal, and anti-inflammatory activities [14-18].

Previous report suggested that RVS shows protective activity in mice models of liver injury established by the administration of carbon tetrachloride [19]. This study focused on the antioxidant property of RVS as a therapeutic mechanism. A recent study demonstrated that butein, a major constituent of RVS, could inhibit ethanol-induced activation of HSC through the TGF-β signaling pathways [20]. Taken together, these results imply that RVS may be useful as a protective agent against different types of liver injuries. However, the roles of RVS in CLC-associated interstitial fibrosis have not been completely understood. The aim of this study was to assess the potential protective effects of RVS and unveil its possible underlying mechanisms in an *in vivo* model of CLC. Herein, we used a rat model of bile duct ligation (BDL) and focused on the involvement of the Smad pathway, a major downstream signaling mediator of TGF-β, as a potential modulatory target of RVS.

Materials and Methods

Preparation of RVS extracts

RVS extract was supplied by Lifetree Biotech Co., Ltd. (Suwon, Korea). The extract was prepared as described previously [21, 22]. In brief, the timber of RVS was harvested in Wonju, Gangwon-do, South Korea, and was cut into 11×1×0.2-cm-sized pieces. These pieces were mixed with water (1:10, w/v) and then eluted with boiling water at 90–110°C for 4 hours. The extract was concentrated to 15% solid content. Next, this concentrated extract was diluted with an equal volume of dextrin, followed by drying using spray-drying method. Urushiol, an allergenic constituent of RVS, was extracted. The urushiol-free RVS extract was authenticated by Korea Advanced Food Research Institute (KAFRI, Seoul, Korea).

Animals

All experiments with rats were acknowledged and regulated by the Institutional Animal Care and Use Committee (IACUC; approved protocol number: P-16-05-A-01) of the Konyang University (Daejeon, Korea). The 8-week-old male Sprague-Dawley rats (n=36; body weight, 185–200 g) were purchased from Samtako (Osan, Korea). The rats were acclimated in an environmentally controlled room at 23±2°C with a 60±10% relative humidity in a 12-hour light/dark cycle, and they had free access to water and food. All experiments were conducted in accordance with the "Guide for the Care and Use of Laboratory Animals" (National Institutes of Health publication 8th edition, 2011).

Experimental design

The rats were randomly divided into the following groups (n=12 per group): sham-surgery (SHAM), BDL, and BDL with RVS-treatment (BDL+RVS) groups. For the BDL+RVS group, RVS (2 mg/kg/day) diluted in distilled water was administered by intragastric route for 28 days (14 days before and after BDL operation). For the BDL group, distilled water as a vehicle was given for 14 days before and after BDL operation. The group of rats receiving laparotomy without ligation of the bile duct was designated as SHAM group. On postoperative day (POD) 14, all the rats were weighed and sacrificed. The livers were removed and some of the tissues were frozen for protein determinations. The remaining tissues were fixed with formalin for histological study. Arterial blood was collected from abdominal aorta for serological assay.

Bile duct ligation

Common bile ducts of each rat were surgically ligated in accordance with the method of Tag et al. [23]. In brief, the rats were anesthetized with a 1:1 mixture (0.2 ml/kg each) of zoletil (Virbac Laboratories, Carros, France) and xylazine

(Kepro, Deventer, The Netherlands). Following laparotomy, common bile duct was isolated and completely occluded with 4-0 black silk. Then, the surgical wound was closed with suture, and the rats were allowed to recover in home cages until they were fully awake and active.

Serological assay

Following the collection of arterial blood, sera were obtained by centrifuge. The sera were stored at −70°C until assayed. The levels of total bilirubin (tBil), direct bilirubin (dBil), aspartate transaminase (AST), and alanine transaminase (ALT) were measured with DRI-CHEM 3000 colorimetric analyzer (Fujifilm, Tokyo, Japan).

Histology

The liver tissues obtained from the right lobe were fixed in 10% neutral buffered formalin and embedded in paraffin. Paraffin blocks were sliced into 5-μm-thick sections on a microtome (RM2255, Leica, Nussloch, Germany). Alterations in the histologic structures of the liver were examined by hematoxylin and eosin (H&E) and Masson's trichrome stain. H&E and Masson's trichrome staining were performed according to previous studies [24, 25]. Two microscopic fields of tissue sections were randomly selected from each rat (n=12 in each group). These fields were photographed at 200× magnification by digital camera connected with light microscope (DM4, Leica) and examined by three blind observers. For assessment of fibrosis degree, the Knodell histology activity index (HAI) was slightly modified and utilized [26]. The following criteria were used in this study: 0, no fibrosis; 1, fibrous expansion of some portal tract with or without short fibrous septa; 2, fibrous expansion of most portal tracts with or without fibrous septa; 3, fibrous expansion of portal tract with occasional portal to portal bridging; 4, fibrous expansion of portal tracts with marked portal to portal as well as portal to central bridging; and 5, marked bridging (portal to portal and/or portal to central) with occasional nodules. Fibrotic areas were measured with the aid of image analysis system (ImageJ software, National Institutes of Health, Bethesda, MD, USA).

Immunofluorescence and immunohistochemistry

To measure the intrahepatic distribution of collagen-I (COL1) and α-smooth muscle actin (α-SMA)–immunopositive myofibroblasts, immunofluorescence (IF) and immunohistochemistry (IHC) were performed respectively. For each rat (n=12 in each group), two randomly selected liver sections were de-paraffinized in xylene, hydrated by immersion in baths featuring a decreasing ethanol gradient, and then washed in distilled water. Next, each section was incubated with primary antibodies that were diluted in blocking solution at a ratio of 1:200 for rabbit anti-COL1 (Santa Cruz Biotechnology, Dallas, TX, USA) and 1:100 for rabbit anti–α-SMA (Santa Cruz Biotechnology) for 24 hours at 4°C. After 3 washes in phosphate buffered saline (PBS), the sections incubated with anti-COL1 and anti–α-SMA were incubated with secondary antibodies containing Cy3-conjugated anti-rabbit IgG and biotinylated anti-rabbit IgG respectively, for 1 hour at room temperature. For IF, the slides were counterstained with mounting medium containing 4′,6-diamidino-2-phenylindole and examined with a confocal laser scanning microscope (LSM700, Zeiss, Munchen, Germany). For IHC, the slides were further incubated with avidin-biotin complex solution for 1 hour at 36°C. The immunopositive regions turned dark brown after the addition of 3,3′-diaminobenzidine tetrahydrochloride (DAB, Sigma-Aldrich, St. Louis, MO, USA) as a chromogen. After cessation of the reaction with DAB, the slides were counterstained with hematoxylin for nuclear staining and examined with a light microscope (Leica).

Western blot analysis

Total protein extraction and western blot analyses were performed as described in a previous study [27]. The liver tissue of each group was gently isolated and transferred to lysis buffer, and homogenized. Randomly chosen five tissue homogenates (n=5 in each group) were incubated with rabbit antibodies against α-SMA (1:1,000), vimentin (1:1,000), phosphorylated Smad3 (1:500), Smad3 (1:500), Smad7 (1:1,000), and glyceraldehyde 3-phosphate dehydrogenase (1:2,000) as primary antibodies. These antibodies were purchased from Santa Cruz Biotechnology. After subsequent incubation with horseradish peroxide–conjugated anti-rabbit IgG (1:1,000, Vector Laboratories, Burlingame, CA, USA) and 5 washes in PBS, the proteins in the polyvinylidene fluoride membranes were detected by a chemiluminescence detection system according to the manufacturer's instructions (ECL, GE Healthcare Life Sciences, Buckinghamshire, UK). The resulting bands were photographed with an imaging device Davinch-K (Davinch-K Corporation, Seoul, Korea). The intensities were quantified with an image analysis system (ImageJ).

Statistical analysis

All data are represented as mean±standard error of the

http://dx.doi.org/10.5115/acb.2016.49.3.189

mean. Comparisons of data from the different groups were performed with one-way analysis of variance (PASW Statistics version 18, SPSS, Inc., Chicago, IL, USA). Differences with *P*-values less than 0.05 were considered to be statistically significant. Each "n" value refers to the number of separate experiments conducted.

Results

RVS normalized the levels of CLC-related serologic parameters altered by BDL

To evaluate the protective effect of RVS in a rat model of BDL-induced CLC, quality of life (QOL)-related general conditions and liver functions were measured in terms of body weight, liver weight, and serologic parameters, such as serum tBil, dBil, AST, and ALT levels (Table 1). Our study revealed that 28 days of RVS administration failed to attenuate CLC-associated QOL deterioration, demonstrating that the loss of body weight induced by BDL was unchanged by RVS. Furthermore, RVS could not normalize the increase of liver weight, associated with the progression of CLC. Notably, tBil and dBil, serum markers of obstructive jaundice, and AST and ALT, serum markers of liver function, were elevated by BDL. The levels of these markers were significantly decreased by RVS treatment on POD 14. This indicated treatment with RVS before and after BDL protects against CLC-associated liver functional damage induced 14 days after BDL.

Table 1. Effect of RVS on BDL-induced alterations in physical and serological parameters

Parameter	SHAM	BDL	BDL+RVS
Body weight (g)	390±21.7	328±17.2[c)]	338±38.2[a)]
Liver weight (g)	13.1±1.4	20.4±1.3[c)]	18.6±1.9[c)]
Liver/Body weight (%)	3.4±0.3	5.9±0.9[c)]	5.6±0.7[c)]
Total bilirubin (mg/dl)	0.4±0.1	9.9±0.8[c)]	6.6±1.9[b),d)]
Direct bilirubin (mg/dl)	0.1±0.0	9.8±1.2[c)]	6.5±1.0[c),d)]
AST (U/l)	50.3±5.5	500.7±76.0[c)]	175.7±42.6[b),e)]
ALT (U/l)	29.0±1.7	167.7±31.5[c)]	67.7±35.3[b),d)]

Values are presented as the mean±SD. RVS, *Rhus verniciflua* Stokes; BDL, bile duct ligation; SHAM, sham-surgery; BDL+RVS, BDL with RVS-treatment; AST, aspartate transaminase; ALT, alanine transaminase. [a)]*P*<0.05, [b)]*P*<0.01, and [c)]*P*<0.001 compared with the SHAM group. [d)]*P*<0.05 and [e)]*P*<0.01 compared with the BDL group.

RVS attenuated CLC-associated histopathological alteration induced by BDL

A representative image of H&E-stained liver tissues, in contrast to normal rat liver morphology is shown in Fig. 1A and D. BDL caused severe histopathological changes such as steatosis, inflammatory cell infiltration (indicated by black arrows), and disarrangement of hepatic cords (Fig. 1B, E). Besides the disruption of tissue architecture, liver fibrosis was identified with fiber extension, large fibrous septa formation, and pseudo-lobe separation. However, these BDL-induced alterations decreased remarkably in the liver sections of rats that received RVS for 14 days before and after treatment (Fig.

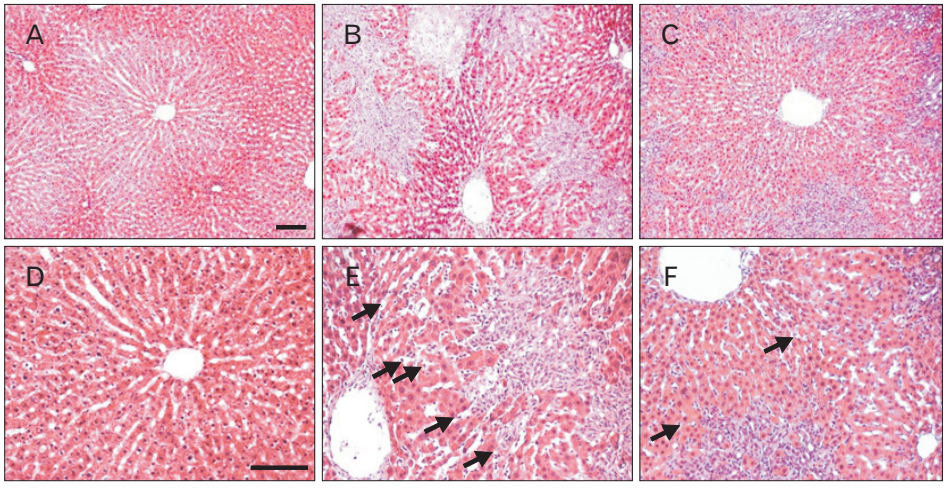

Fig. 1. Protective effect of *Rhus verniciflua* Stokes (RVS) on bile duct ligation (BDL)–induced hepatic parenchymal injury. Rats (n=12 in each group) were pretreated with RVS (2 mg/kg) for 14 days, followed by BDL operation with RVS (2 mg/kg) for additional 14 days. Sham-surgery (SHAM) group underwent the same procedures except the actual ligation of the common bile duct. BDL group was administered distilled water as a vehicle. Representative photomicrographs are H&E stained tissue sections of SHAM (A, D), BDL (B, E), and BDL with RVS-treatment (BDL+RVS) groups (C, F) with low (A–C) and high magnification (D–F). The black arrows indicates infiltrated inflammatory cells. Scale bars=100 μm.

1C, F). This indicated that RVS might prevent or resolve CLC-related histologic alterations in the liver.

RVS attenuated CLC-associated ECM deposition induced by BDL

To evaluate the degree of liver fibrosis on POD 14 in different groups, the extent of ECM deposition was studied

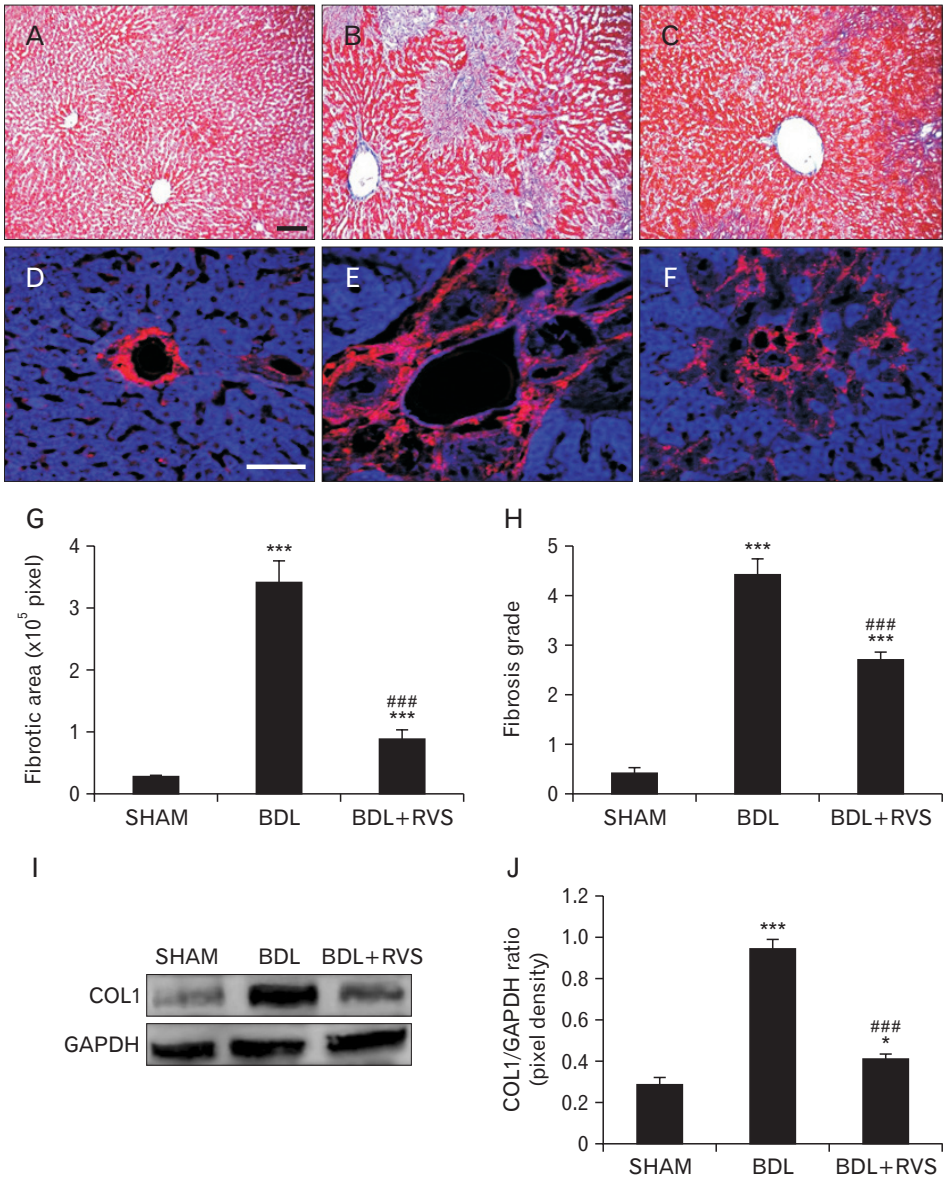

Fig. 2. Attenuation of bile duct ligation (BDL)–induced hepatic interstitial fibrosis by *Rhus verniciflua* Stokes (RVS) treatment. Rats (n=12 in each group) were pretreated with RVS (2 mg/kg) for 14 days, followed by BDL operation with RVS (2 mg/kg) for additional 14 days. Sham-surgery (SHAM) group underwent the same procedures except the actual ligation of the common bile duct. BDL group was administered distilled water as a vehicle. Representative photomicrographs in upper panel are Masson's trichrome-stained tissue sections of SHAM (A), BDL (B), and BDL with RVS-treatment (BDL+RVS) groups (C). Scale bar=100 μm (A–C). Photomicrographs in the lower panel are fluorescent images captured under laser confocal microscope, showing collagen-I (COL1) immunoreactivities (appeared red) in liver tissue sections of SHAM (D), BDL (E), and BDL+RVS groups (F). Scale bar=100 μm (D–F). Fibrotic area (G) was measured by the averaged area of blue pixels within each of the Masson's trichrome-stained liver tissue. The degree of fibrosis (H) was graded according to the modification of Knodell histology activity index using Masson's trichrome-stained liver sections. The amount of COL1 in liver homogenates of each group was assessed by immunoblots, and the resulting representative blot images (I) and quantitative graphs (J) are shown. Glyceraldehyde 3-phosphate dehydrogenase (GAPDH) was used as a loading control (n=5; *P<0.05 and ***P<0.001 compared with the SHAM group; $^{###}P$<0.001 compared with the BDL group). Data in all graphs are expressed as the mean±SD.

http://dx.doi.org/10.5115/acb.2016.49.3.189

through Masson's trichrome staining. As shown in representative images (Fig. 2A–C) and quantitative graphs for fibrotic area (Fig. 2G), the liver tissue of BDL group displayed a large area of ECM deposition, whereas that of BDL+RVS group showed markedly diminished area (89,922±38,721 vs. 342,536±97,302, P<0.001). Fibrosis degree (Fig. 2H), which was quantified by the modification of Knodell HAI criteria, was also increased in the BDL group compared to that in the SHAM group. However, the fibrosis degree of BDL+RVS group remarkably decreased when compared to that of the BDL group (2.7±0.50 vs. 4.42±0.78, P<0.001). Based on the notion that COL1 is the dominant constituent of ECM, we performed distributional (Fig. 2D–F) and semi-quantitative assessment (Fig. 2I, J) of COL1 in the livers of different groups. Compared to the SHAM group, the amount of COL1 in the liver tissue and tissue homogenates of BDL group markedly increased. The hepatic deposition of COL1 significantly decreased morphologically and semi-quantitatively in the BDL+RVS group compared with that in the BDL group (0.41±0.03 vs. 0.94±0.08, P<0.001). These results revealed that RVS might be useful in preventing or resolving liver fibrosis due to CLC.

RVS inhibited myofibroblast activation induced by BDL

As ECM is mainly synthesized by interstitial myofibroblasts, we tested whether the antifibrotic effects of RVS might

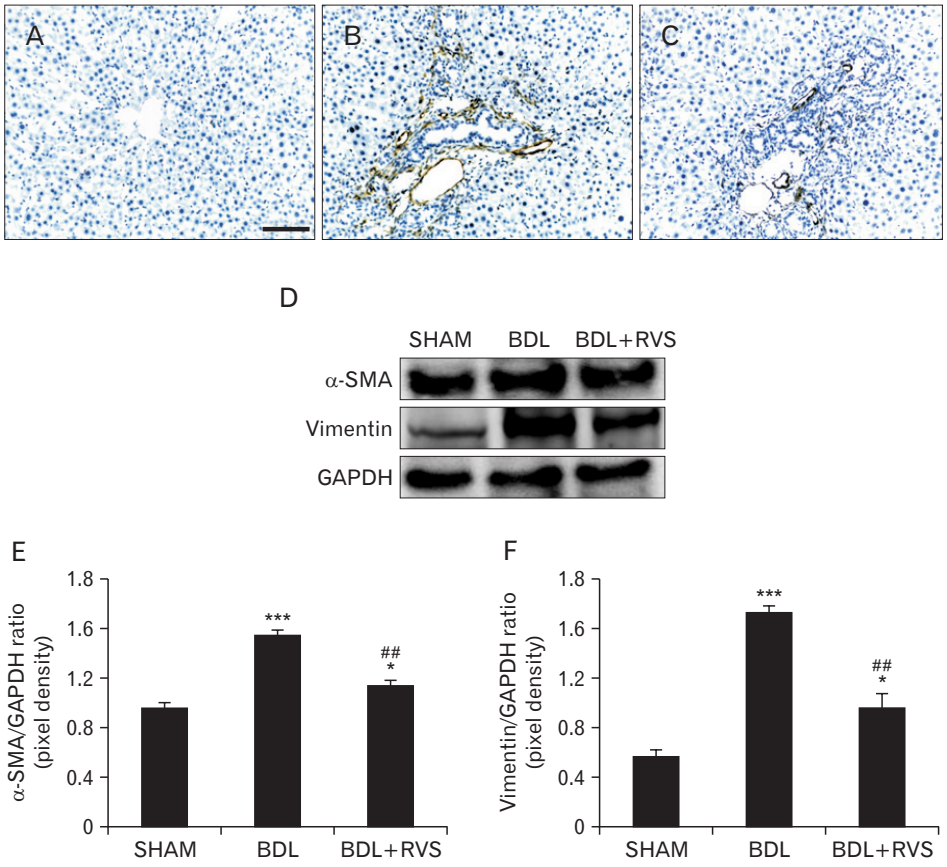

Fig. 3. Attenuation of bile duct ligation (BDL)–induced myofibroblast activation by *Rhus verniciflua* Stokes (RVS) treatment. Rats (n=12 in each group) were pretreated with RVS (2 mg/kg) for 14 days followed by BDL operation with RVS (2 mg/kg) for additional 14 days. Sham-surgery (SHAM) group underwent the same procedures except the actual ligation of the common bile duct. BDL group was administered distilled water as a vehicle. Representative images of immunohistochemistry staining for α-smooth muscle actin (α-SMA; appeared brown) in the liver tissue sections of SHAM (A), BDL (B), and BDL with RVS-treatment (BDL+RVS) groups (C) are shown. Nuclei (appeared purple) were counterstained by hematoxylin. Scale bar=100 μm. The amount of α-SMA and vimentin in liver homogenates was assessed by immunoblots. The representative blot images (D) and quantitative graphs revealing α-SMA (E) and vimentin (F) expression are shown. Glyceraldehyde 3-phosphate dehydrogenase (GAPDH) was used as a loading control (n=5; $^{*}P$<0.05 and $^{***}P$<0.001 compared with the SHAM group; $^{\#\#}P$<0.01 compared with the BDL group). Data in both graphs are expressed as the mean±SD.

be due to the inhibition of myofibroblast activation. For this purpose, IHC for α-SMA, a well-known marker of activated myofibroblast, was performed using liver tissue from different groups. In the SHAM group, α-SMA–immunopositive cells were hardly observed in liver parenchyma as well as in the portal areas (Fig. 3A). In the BDL group (Fig. 3B), numerous α-SMA–positive myofibroblasts were observed in the liver around the dilated ducts in the portal areas. However, the amount of these cells markedly decreased in the liver tissue of BDL+RVS group (Fig. 3C). Immunoblots also revealed that the levels of α-SMA and vimentin, another well-known marker of myofibroblast, dramatically increased in the BDL group compared with those in SHAM group (1.54±0.07 vs. 0.96±0.03 and 1.73±0.08 vs. 0.57±0.08, respectively, $P<0.001$). These levels were significantly decreased by the 28-day treatment with RVS (1.14±0.08 and 0.97±0.17, $P<0.01$ vs. BDL) (Fig. 3D–F). These findings indicated that the antifibrotic effect of RVS might be, at least partly, due to the inhibition of hepatic myofibroblast activation.

RVS inhibited profibrotic Smad3 signaling by Smad7 upregulation

Smad3 signaling is a key pathway leading to liver fibrosis upon stimulation by TGF-β, a major profibrotic cytokine that derived from various sources. Therefore, we investigated the mechanisms by which RVS attenuates BDL-induced CLC by examining the signaling pathway of Smad3 and its inhibitory regulator Smad7. We demonstrated that BDL group exhibited a marked upregulation of *p*-Smad3/Smad3 ratio (1.74±0.07 vs. 0.79±0.12, $P<0.001$) as well as a decreased level of Smad7 compared with SHAM group (0.37±0.12 vs. 0.6±0.03, $P<0.001$) (Fig. 4A–C). Notably, BDL+RVS group showed a significant reduction of *p*-Smad3 and an increase of Smad7 levels compared with the BDL group (1.74±0.07 vs. 0.67±0.1 and 1.71±0.07 vs. 0.37±0.12, $P<0.001$). This indicated that the inhibitory effect of RVS on myofibroblast activation might be due to the downregulation of Smad3 and reciprocal upregulation of Smad7 in liver tissue.

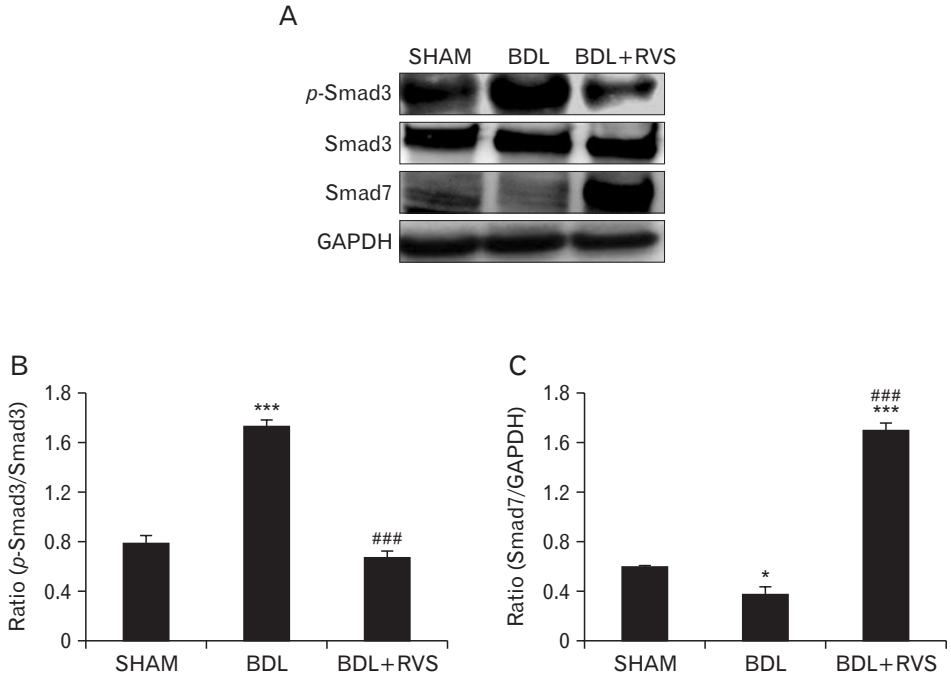

Fig. 4. Effects of *Rhus verniciflua* Stokes (RVS) on bile duct ligation (BDL)–induced alterations in *p*-Smad3/Smad3 ratio and amount of Smad7 in liver homogenates. Rats (n=12 in each group) were pretreated with RVS (2 mg/kg) for 14 days followed by BDL operation with RVS (BDL+RVS, 2 mg/kg) for additional 14 days. Sham-surgery (SHAM) group underwent the same procedures except the actual ligation of the common bile duct. BDL group was administered distilled water as a vehicle. The amount of *p*-Smad3, Smad3, and Smad7 in the liver homogenates of different groups was assessed by immunoblots. The representative blot images (A) and quantitative graphs revealing *p*-Smad3/Smad3 ratio (B) and Smad7 (C) expression are shown. Smad3 and glyceraldehyde 3-phosphate dehydrogenase (GAPDH) were used as loading controls in panels (B) and (C), respectively (n=5; $^{*}P<0.05$ and $^{***}P<0.001$ compared with the SHAM group; $^{\#\#\#}P<0.01$ compared with the BDL group). Data in both graphs are expressed as the mean±SD.

http://dx.doi.org/10.5115/acb.2016.49.3.189

Discussion

Clinical studies and studies on animal models have been carried out to analyze the effects of administration of various synthetic drugs on liver fibrosis associated with or without CLC [28, 29]. To date, however, these studies were not able to suggest definitive solutions regarding the beneficial or hazardous effect of therapeutic usage [30, 31]. On the other hand, many traditional medicines and their natural products in Asian countries are known to be relatively low priced and effective resources for drug development, and identified with very little noxious effects in clinical situations involving hepatobiliary diseases [32]. It seems that the benefits far outweigh the potential risks, such as poisoning, nephrotoxicity, and acute hepatotoxicity, to the patient [33, 34]. Thus, the therapeutic screening of natural plant extracts in this situation may be reasonable.

RVS, which has been used for thousands of years in Asian countries, is one of the remedies against liver injuries. RVS is a tree species of genus *Toxicodendron* belonging to the family *Anacardiaceae* and is grown in regions of China and Korea [35, 36]. In Korea, RVS has been used as a therapeutic for digestive problems such as gastritis and abdominal masses since the ancient times [37]. RVS has also been used as a food additive. However, there is lack of scientific evidence proving these health benefits of RVS. Recently, a body of *in vitro* studies for RVS has emerged to reveal its potential antibacterial, antimicrobial, antirheumatoid, anti-inflammatory, antioxidant, antiaggregation, anticancer, and neuroprotective activities [38-42]. The effects of RVS on these entities in hepatobiliary diseases have been demonstrated by few approaches. RVS has been shown to suppress aflatoxin B1-induced increase in serum levels of ALT, alkaline phosphatase, and lactate dehydrogenase, prevent malondialdehyde formation, and inhibit the decrease in the levels of glutathione and superoxide dismutase in a mouse model [43]. In another study, RVS protected against liver damage through the inhibition of radical scavenging ability [44]. A study performed by Park et al. [45] proposed for the first time that methanol and ethyl acetate extract of RVS and two active compounds of RVS, sulfuretin and fustin, have a protective effect in experimental models of CLC. According to their reports, these compounds exerted hepatoprotective effects via the augmentation of the liver antioxidant defense system. Herein, we suggested the beneficial effects of RVS on CLC using different approaches.

Unlike in the study by Choi et al. [43], we focused on myofibroblast activation and its master signaling regulator, TGF-β/Smad pathway, possibly involved in the CLC pathogenesis. In this study, we demonstrated that BDL markedly elevated the levels of AST, ALT, tBil, and dBil, all of which were significantly attenuated by the 28-day treatment with RVS (2 mg/kg/day).We also observed the protection of liver histoarchitecture and inhibition of excessive deposition of ECM by RVS treatment. We observed that RVS inhibited BDL-induced proliferation and activation of interstitial myofibroblast, and these effects were strongly associated with the inactivation of Smad3 and reciprocal upregulation of Smad7.

However, we cannot rule out the possibility that RVS might exert protective effects on CLC by another mechanism. In fact, numerous factors that can be possible targets of RVS exist in the pathogenesis of CLC-induced liver fibrosis. All hepatic parenchymal cells undergo specific changes in the progression towards liver fibrosis. For example, the hepatocytes are injured and they undergo apoptosis and eventually necrosis [46, 47]. The endothelial cells in sinusoidal capillary undergo a loss of fenestrae and intercellular integrity [48]. The Kupffer cells, which are the resident macrophages in the liver, activate and secrete various chemokines and cytokines [49, 50]. The lymphocytes infiltrate the damaged liver and contribute to the inflammatory process. Finally, the quiescent HSC are activated to produce ECM [51, 52]. Thus, based on the biological properties of RVS such as anti-apoptotic, angioprotective, anti-inflammatory, and antifibrotic effects, it was suggested that RVS might exert beneficial effects on CLC by multifactorial mechanisms. Therefore, by using single compounds within RVS, approaches for unveiling other therapeutic mechanisms and specific molecular targets might be needed in the context of protective effects of RVS on CLC.

Acknowledgements

This study was supported by the Development of Forest Science and Technology (grant numbers S111414L030100) and the Korea Research Foundation (grant numbers NRF-2014R1A1A403005726 and -2016R1C1B2012351).

References

1. Feld JJ, Heathcote EJ. Epidemiology of autoimmune liver disease. J Gastroenterol Hepatol 2003;18:1118-28.
2. Iredale JP. Cirrhosis: new research provides a basis for rational and targeted treatments. BMJ 2003;327:143-7.
3. Schuppan D, Ruehl M, Somasundaram R, Hahn EG. Matrix as a modulator of hepatic fibrogenesis. Semin Liver Dis 2001;21:351-72.

4. Bataller R, Brenner DA. Liver fibrosis. J Clin Invest 2005;115:209-18.
5. Friedman SL. Mechanisms of hepatic fibrogenesis. Gastroenterology 2008;134:1655-69.
6. Sasaki T, Ohta S, Kamogawa A, Shinoda M. Protective effects of various Chinese traditional medicines against experimental cholestasis. Chem Pharm Bull (Tokyo) 1990;38:513-6.
7. Dooley S, Hamzavi J, Breitkopf K, Wiercinska E, Said HM, Lorenzen J, Ten Dijke P, Gressner AM. Smad7 prevents activation of hepatic stellate cells and liver fibrosis in rats. Gastroenterology 2003;125:178-91.
8. Dooley S, Hamzavi J, Ciuclan L, Godoy P, Ilkavets I, Ehnert S, Ueberham E, Gebhardt R, Kanzler S, Geier A, Breitkopf K, Weng H, Mertens PR. Hepatocyte-specific Smad7 expression attenuates TGF-beta-mediated fibrogenesis and protects against liver damage. Gastroenterology 2008;135:642-59.
9. Meindl-Beinker NM, Dooley S. Transforming growth factor-beta and hepatocyte transdifferentiation in liver fibrogenesis. J Gastroenterol Hepatol 2008;23 Suppl 1:S122-7.
10. Kershenobich Stalnikowitz D, Weissbrod AB. Liver fibrosis and inflammation: a review. Ann Hepatol 2003;2:159-63.
11. Szabo G, Mandrekar P, Dolganiuc A. Innate immune response and hepatic inflammation. Semin Liver Dis 2007;27:339-50.
12. Luper S. A review of plants used in the treatment of liver disease: part 1. Altern Med Rev 1998;3:410-21.
13. Kitts DD, Lim KT. Antitumorigenic and cytotoxic properties of an ethanol extract derived from *Rhus verniciflua* Stokes (RVS). J Toxicol Environ Health A 2001;64:357-71.
14. Lim KT, Hu C, Kitts DD. Antioxidant activity of a *Rhus verniciflua* Stokes ethanol extract. Food Chem Toxicol 2001;39:229-37.
15. Jeon WK, Kim JH, Lee HW, Ko BS, Kim HK. Effects of *Rhus verniciflua* Stokes (RVS) extract on diet-induced obesity in C57BL/6 mouse. Korean J Pharmacogn 2003;34:339-43.
16. Kim MJ, Choi WC, Barshinikov AM, Kobayashi A. Anticancer and antioxidant activity of allergen-removed extract in *Rhus verniciflua* Stokes. Korean J Med Crop Sci 2002;10:288-93.
17. Kim IT, Park YM, Shin KM, Ha J, Choi J, Jung HJ, Park HJ, Lee KT. Anti-inflammatory and anti-nociceptive effects of the extract from *Kalopanax pictus*, *Pueraria thunbergiana* and *Rhus verniciflua*. J Ethnopharmacol 2004;94:165-73.
18. Park KY, Jung GO, Lee KT, Choi J, Choi MY, Kim GT, Jung HJ, Park HJ. Antimutagenic activity of flavonoids from the heartwood of *Rhus verniciflua*. J Ethnopharmacol 2004;90:73-9.
19. Ko JH, Lee SJ, Lim KT. *Rhus verniciflua* Stokes glycoprotein (36kDa) has protective activity on carbon tetrachloride-induced liver injury in mice. Environ Toxicol Pharmacol 2006;22:8-14.
20. Szuster-Ciesielska A, Mizerska-Dudka M, Daniluk J, Kandefer-Szerszeń M. Butein inhibits ethanol-induced activation of liver stellate cells through TGF-beta, NFkappaB, p38, and JNK signaling pathways and inhibition of oxidative stress. J Gastroenterol 2013;48:222-37.
21. Han QB, Song JZ, Qiao CF, Wong L, Xu HX. Preparative separation of gambogic acid and its C-2 epimer using recycling high-speed counter-current chromatography. J Chromatogr A 2006;1127:298-301.
22. Kim SA, Kim SH, Kim IS, Lee D, Dong MS, Na CS, Nhiem NX, Yoo HH. Simultaneous determination of bioactive phenolic compounds in the stem extract of *Rhus verniciflua* stokes by high performance liquid chromatography. Food Chem 2013;141:3813-9.
23. Tag CG, Sauer-Lehnen S, Weiskirchen S, Borkham-Kamphorst E, Tolba RH, Tacke F, Weiskirchen R. Bile duct ligation in mice: induction of inflammatory liver injury and fibrosis by obstructive cholestasis. J Vis Exp 2015;(96):52438.
24. Fischer AH, Jacobson KA, Rose J, Zeller R. Hematoxylin and eosin staining of tissue and cell sections. CSH Protoc 2008;2008:pdb.prot4986.
25. Goldner J. A modification of the masson trichrome technique for routine laboratory purposes. Am J Pathol 1938;14:237-43.
26. Knodell RG, Ishak KG, Black WC, Chen TS, Craig R, Kaplowitz N, Kiernan TW, Wollman J. Formulation and application of a numerical scoring system for assessing histological activity in asymptomatic chronic active hepatitis. Hepatology 1981;1:431-5.
27. Kim JH, Yu KS, Jeong JH, Lee NS, Lee JH, Jeong YG, Yoo YC, Han SY. All-trans-retinoic acid rescues neurons after global ischemia by attenuating neuroinflammatory reactions. Neurochem Res 2013;38:2604-15.
28. Rigato I, Cravatari M, Avellini C, Ponte E, Crocè SL, Tiribelli C. Drug-induced acute cholestatic liver damage in a patient with mutation of UGT1A1. Nat Clin Pract Gastroenterol Hepatol 2007;4:403-8.
29. Shah B, Shah G. Antifibrotic effect of heparin on liver fibrosis model in rats. World J Gastrointest Pharmacol Ther 2012;3:86-92.
30. Scott S, Thompson J. Adverse drug reactions. Anaesth Intensive Care Med 2014;15:245-9.
31. Kashaw V, Nema AK, Agarwal A. Hepatoprotective prospective of herbal drugs and their vesicular carriers: a review. Int J Res Pharm Biomed Sci 2011;2:360-74.
32. Zhang A, Sun H, Wang X. Recent advances in natural products from plants for treatment of liver diseases. Eur J Med Chem 2013;63:570-7.
33. Balandrin MF, Klocke JA, Wurtele ES, Bollinger WH. Natural plant chemicals: sources of industrial and medicinal materials. Science 1985;228:1154-60.
34. Srivastava J, Lambert J, Vietmeyer N. Medicinal plants: an expanding role in development. World Bank Technical Paper 320. Washington, DC: World Bank Publications;1996.
35. Kim TJ. Korean resource plants. Vol. II. Seoul: Seoul National University Press; 1996. p.292-7.
36. Hong DH, Han SB, Lee CW, Park SH, Jeon YJ, Kim MJ, Kwak SS, Kim HM. Cytotoxicity of urushiols isolated from sap of Korean lacquer tree (*Rhus vernicifera* Stokes). Arch Pharm Res 1999;22:638-41.
37. Namba T. Coloured illustrations of Wakan-Yaku. Osaka: Hoikusha Publishing Co.; 1980.
38. Lee JC, Kim J, Lim KT, Yang MS, Jang YS. Ethanol eluted extract of *Rhus verniciflua* Stokes showed both antioxidant and cytotoxic effects on mouse thymocytes depending on the dose and time of

http://dx.doi.org/10.5115/acb.2016.49.3.189

the treatment. BMB Rep 2001;34:250-8.
39. Lee JC, Lim KT. Screening of antioxidant and antimicrobial effects from *Rhus verniciflua* Stokes (RVS) ethanolic extract. Food Sci Biotechnol 2000;9:139-45.
40. Lee JD, Huh JE, Jeon G, Yang HR, Woo HS, Choi DY, Park DS. Flavonol-rich RVHxR from *Rhus verniciflua* Stokes and its major compound fisetin inhibits inflammation-related cytokines and angiogenic factor in rheumatoid arthritic fibroblast-like synovial cells and *in vivo* models. Int Immunopharmacol 2009;9:268-76.
41. Lee JC, Jung HY, Lim KT. Effects of *Rhus verniciflua* Stokes (RVS) on the plasma level of cholesterol and tumor growth in mouse. J Toxicol Public Health 1999;15:169-75.
42. Cho N, Choi JH, Yang H, Jeong EJ, Lee KY, Kim YC, Sung SH. Neuroprotective and anti-inflammatory effects of flavonoids isolated from *Rhus verniciflua* in neuronal HT22 and microglial BV2 cell lines. Food Chem Toxicol 2012;50:1940-5.
43. Choi KC, Chung WT, Kwon JK, Jang YS, Yu JY, Park SM, Lee JC. Chemoprevention of a flavonoid fraction from *Rhus verniciflua* Stokes on aflatoxin B1-induced hepatic damage in mice. J Appl Toxicol 2011;31:150-6.
44. Lee JC, Lim KT, Jang YS. Identification of *Rhus verniciflua* Stokes compounds that exhibit free radical scavenging and anti-apoptotic properties. Biochim Biophys Acta 2002;1570:181-91.
45. Park HJ, Lee KT, Park KY, Han GY, Jung MH, Choi J. Protective mechanism of flavonoids isolated from *Rhus verniciflua* on the biliary liver fibrosis in rat. Korean J Life Sci 2002;12:332-9.
46. Faubion WA, Guicciardi ME, Miyoshi H, Bronk SF, Roberts PJ, Svingen PA, Kaufmann SH, Gores GJ. Toxic bile salts induce rodent hepatocyte apoptosis via direct activation of Fas. J Clin Invest 1999;103:137-45.
47. Patel T, Bronk SF, Gores GJ. Increases of intracellular magnesium promote glycodeoxycholate-induced apoptosis in rat hepatocytes. J Clin Invest 1994;94:2183-92.
48. Fernández M, Semela D, Bruix J, Colle I, Pinzani M, Bosch J. Angiogenesis in liver disease. J Hepatol 2009;50:604-20.
49. Zavadil J, Bottinger EP. TGF-beta and epithelial-to-mesenchymal transitions. Oncogene 2005;24:5764-74.
50. Hernandez-Gea V, Friedman SL. Pathogenesis of liver fibrosis. Annu Rev Pathol 2011;6:425-56.
51. Maher JJ. Interactions between hepatic stellate cells and the immune system. Semin Liver Dis 2001;21:417-26.
52. Mehal WZ, Friedman SL. The role of inflammation and immunity in the pathogenesis of liver fibrosis. In: Gershwin ME, Vierling JM, Manns MP, editors. Liver Immunology. Totowa, NJ: Humana Press; 2007. p.111-21.